PPPL-2272
UC20-F,G

PPPL-2272

NUMERICAL MODELING OF LOWER HYBRID HEATING AND CURRENT DRIVE

By

E.J. Valeo and D.C. Eder

MARCH 1986

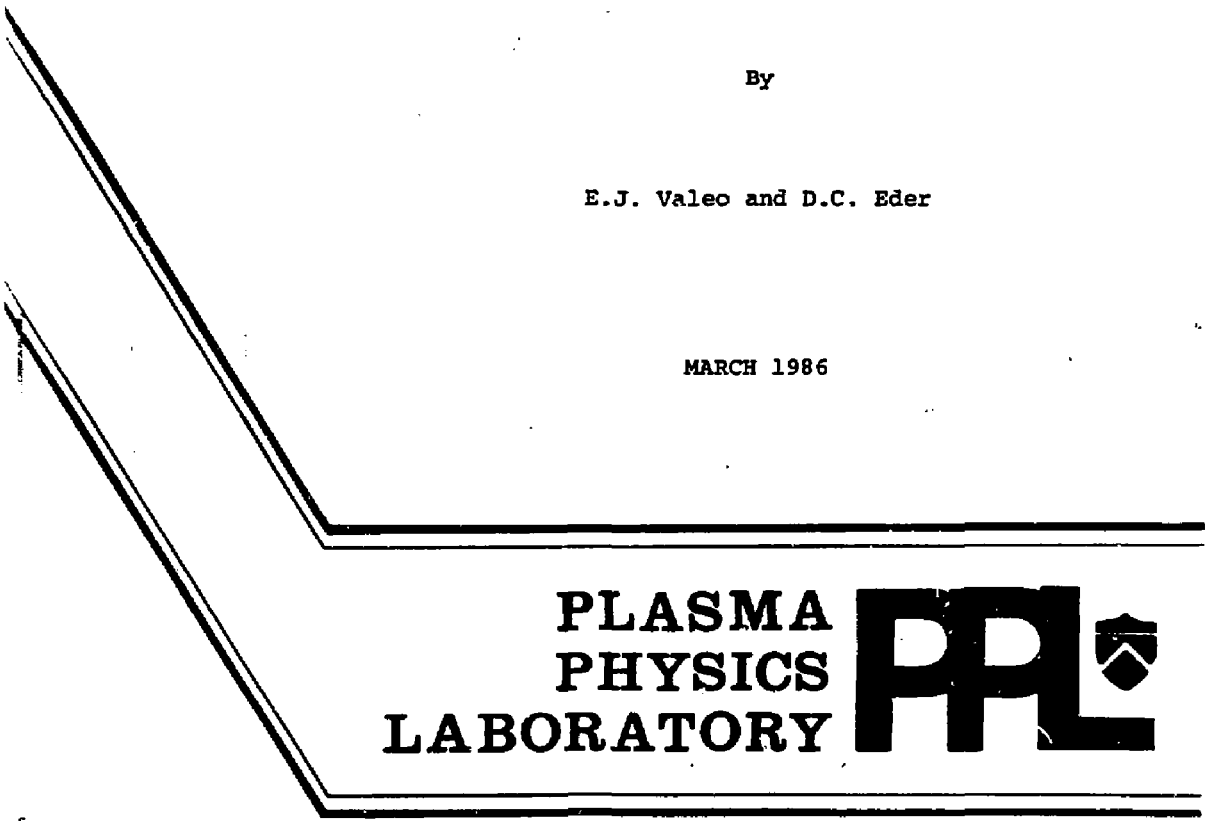

PRINCETON UNIVERSITY
PRINCETON, NEW JERSEY

PREPARED FOR THE U.S. DEPARTMENT OF ENERGY,
UNDER CONTRACT DE-AC02-76-CHO-3073.

PPPL--2272

DE86 009750

Numerical Modeling of Lower Hybrid Heating and Current Drive

Ernest J. Valeo and David C. Eder*
Plasma Physics Laboratory, Princeton University
P.O. Box 451, Princeton
New Jersey 08544, U.S.A.

The generation of currents in toroidal plasma by application of waves in the lower hybrid frequency range involves the interplay of several physical phenomena which include: wave propagation in toroidal geometry, absorption via wave-particle resonances, the quasilinear generation of strongly nonequilibrium electron and ion distribution functions, and the self-consistent evolution of the current density in such a nonequilibrium plasma. We describe a code, LHMOD, which we have developed to treat these aspects of current drive and heating in tokamaks. We present results obtained by applying the code to a computation of current ramp-up and to an investigation of the possible importance of minority hydrogen absorption in a deuterium plasma as the "density limit" to current drive is approached.

*Present Address: University of California, Lawrence Livermore National National Laboratory, P.O. Box 808, Livermore, California 94550, U.S.A

I. Introduction

Fisch's theoretical proposal[1] that distortions in the electron distribution function driven by externally injected waves could be used to sustain current in a laboratory plasma, and the subsequent encouraging experimental observation of this effect[2–4] has motivated substantial additional theoretical and experimental effort. Indeed, a steady-state tokamak reactor[5,6] becomes a possibility if inductive current drive is supplanted by rf current drive.

Because the particle distribution functions in an rf-driven plasma are strongly distorted from a Maxwellian shape, the near-equilibrium assumption which forms the basis for the description employed in transport modeling codes is inappropriate. A quantitative description requires incorporation of kinetic effects. One recent approach[7] is to construct a constitutive relation between the (time dependent) current density and the inductive electric field, which is modified from the simple linear relation $\mathcal{E} = \eta j$ by the velocity space flux due to an (assumed known) wave spectrum. An alternative approach,[8] in which a reduced (model) kinetic equation is solved, together with evolution equations for the wave spectrum and for the current density, is described here. This approach is similar in many respects to that employed by Bonoli and coworkers at MIT.[9]

The overall structure of our code, LHMOD, is described in Section II. In Sections III through V the principal modules are described in some detail. Two applications of the code are described in Section VI. The first is a study of current ramp-up in a plasma of sufficiently low density so that $\omega_{LH} \ll \omega_{rf}$ everywhere. The second focusses on the role of minority hydrogen absorption in a deuterium plasma as the density is raised and $\omega_{LH} \rightarrow \omega_{rf}$ at the plasma center. The results suggest that minority hydrogen ion absorption could play a role in determining the observed "density limit" to current drive.

II. Framework of the Modeling Code

The code LHMOD consists of three strongly coupled modules which deal with the physical processes of

1) Wave propagation and absorption,
2) Computation of the electron and ion distribution functions,
3) Evolution of the plasma current.

These modules are described in detail in Sections III through V. Here we briefly discuss the overall structure and the strongly interrelated nature of the computations.

Wave propagation is described by the warm plasma, fully electromagnetic ray equations. Energy deposition and current drive occur principally through the resonant wave-particle interaction. The resonant electron interaction is with the parallel wave electric field and the ion interaction is through the perpendicular wave electric

field. The linear approximation is assumed to describe adequately the interaction in both cases.

If the wave amplitudes were sufficiently weak so that the particle distribution functions maintained their Maxwellian shape, then the damping calculations would be trivial. However, under conditions of significant heating or current drive, the Coulomb collisional relaxation toward a Maxwellian is completely dominated by the wave-driven quasilinear diffusion. The local velocity space gradient, $\nabla_v f$, which determines the damping decrement, consequently, depends on the entire wave spectrum. One is therefore led to introduce additional equations for the evolution of f_e and f_i which are to be solved on a par with the wave equations.

Consideration of even the relatively simple case in which the inductive electric field vanishes ("steady state") illustrates how tightly coupled these calculations are in general. The problem is that, unless one is willing to follow the evolution of the system on the exceedingly short time scale $\tau_{convection} \approx a/v_{gr,r}$, with $v_{gr,r}$ the radial component of the wave group velocity, there is no obvious timelike variable which allows one to advance the coupled wave-particle system to a steady state. The radial coordinate would serve this role if total absorption occurred during the first inward pass. Unfortunately, this is a rather special class of solutions. More generally, one finds that the waves undergo several radial excursions before complete absorption occurs. Since, as shown below, the flux-surface-averaged wave energy density versus wave vector determines the incremental absorption at each flux surface, one is forced to an interative solution of the coupled set of wave and kinetic equations.

The situation becomes more complicated still if the poloidal flux is allowed to evolve. The difficulty here is that the inductive electric field is determined locally at each radius by the constraint that, for times short compared to the L/R time for the plasma, the current density is conserved. This constraint is enforceable only upon solution of the electron kinetic equation and direct computation of $j_\parallel$. We are thus led to a second iteration process, this time to determine $\mathcal{E}[j(r,t)]$ and the associated nonlinear conductivity, $\partial j/\partial E$, which appears in the flux diffusion equation.

III. Wave Propagation and Absorption

Because their wavelength is small compared to characteristic gradient scale lengths in tokamaks, the propagation of lower hybrid waves is well described by the ray approximation. We briefly review the underlying theory, partially for the purpose of introducing notation and definitions required later. Assuming local homogeneity and strict time independence of the plasma medium, we introduce the eikonal representation

$$A(\mathbf{x},t) \propto exp(i\int^{\mathbf{x}} d\mathbf{x}' \cdot \mathbf{k}(\mathbf{x}') - i\omega t) \quad , \tag{1}$$

for the time and space variation of field amplitudes with frequency ω and local wave vector $\mathbf{k}$. The plasma dielectric tensor $\mathbf{K}$ relates the plasma current $\mathbf{j}$ and the

displacement vector $\mathbf{D}$ to the wave electric field as follows

$$\mathbf{D} = \mathbf{K} \cdot \mathbf{E} = \mathbf{E} + \frac{4\pi i}{\omega}\mathbf{j} \quad . \tag{2}$$

The general expression for $\mathbf{K}$ in a hot, magnetized plasma[10] simplifies enormously in the lower hybrid frequency range if one makes use of the well-satisfied inequalities

$$\omega \ll \Omega_e, \qquad k_\perp \rho_e \ll 1 \quad , \tag{3a}$$

$$\omega \gg \Omega_i, \qquad k_\perp \rho_i \gg 1 \quad . \tag{3b}$$

The set of inequalities Eq.(3b), together with the invokation of a mechanism which randomizes the wave phase as seen by the plasma ions[13] allows the use of the approximation $B \to 0$ in the calculation of the ion response. If, as we assume, the waves have sufficiently large phase speed both along and across the magnetic field, i.e., $\omega/k_\parallel v_{Te}$ and $\omega/k_\perp v_{Ti}$ are sufficiently large, then the dielectric tensor is almost Hermetian, and the contribution of the anti-Hermetian part (which yields energy deposition by the waves into the plasma) can be calculated as a correction term. With these approximations, the dielectric tensor $\mathbf{K}$ is expressible in Cartesian coordinates (x, y, z), locally chosen so that $\hat{\mathbf{z}} \wedge \mathbf{B} = 0$, $\mathbf{k} = \hat{\mathbf{x}}k_\perp + \hat{\mathbf{z}}k_\parallel$, as

$$\mathbf{K} = K_{xx}\hat{\mathbf{x}}\hat{\mathbf{x}} + K_{yy}\hat{\mathbf{y}}\hat{\mathbf{y}} + iK_{xy}(\hat{\mathbf{x}}\hat{\mathbf{y}} - \hat{\mathbf{y}}\hat{\mathbf{x}}) + K_{zz}\hat{\mathbf{z}}\hat{\mathbf{z}} \quad , \tag{4}$$

where

$$K_{xx} = K_\perp + iK_{xx,i} \quad . \tag{5a}$$

$$K_{yy} = K_\perp + iK_{yy,i} \quad . \tag{5b}$$

$$K_{xy} = \frac{\omega_{pe}^2}{\omega\Omega_e} + iK_{xy,i} \quad . \tag{5c}$$

$$K_{zz} = K_\parallel + iK_{\parallel,i} \quad , \tag{5d}$$

with

$$K_\perp = 1 + \frac{\omega_{pe}^2}{\Omega_e^2} - \frac{\omega_{pi}^2}{\omega^2} - k_\perp^2 K_{Th} \quad . \tag{5e}$$

$$K_\parallel = 1 - \frac{\omega_{pe}^2}{\omega^2} \quad . \tag{5f}$$

and where

$$K_{Th} = \frac{3}{4}\frac{\omega_{pe}^2}{\Omega_e^4}v_{Te}^2 + 3\sum_j \frac{\omega_{pi,j}^2 v_{Ti,j}^2}{\omega^4} \quad . \tag{5g}$$

The anti-Hermitian part $\mathbf{K}_a$ of $\mathbf{K}$, which arises from the resonant wave particle interaction, assumes the general form

$$\mathbf{K}_a = \mathrm{Imag} \sum_j \frac{\omega_{pj}{}^2}{\omega} \int d^3v\, \mathbf{v} \frac{\partial f_{i,j}/\partial \mathbf{v}}{\omega - \mathbf{k}\cdot\mathbf{v} + i\delta} \quad . \tag{6}$$

In the parallel direction, the electron interaction dominates with the result

$$K_{\parallel,i} = \pi\frac{\omega_{pe}^2}{\omega}\int dv_\parallel v_\parallel \frac{\partial f_e}{\partial v_\parallel}\delta(\omega - k_\parallel v_\parallel).$$

$$= \pi \left(\frac{\omega_{pe}}{k_\parallel}\right)^2 \frac{\partial f_e}{\partial v_\parallel}\Big|_{v_\parallel = \omega/k_\parallel} \quad . \tag{7}$$

The ions dominate the anti-Hermetian contribution perpendicular to **B**. Making the plausible assumption that the strong magnetic field isotropizes f_i so that $f_i(\mathbf{v}_\perp) = f_i(v_\perp)$, the off-diagonal contributions to $\mathbf{K}_a$ vanish. Then the projection of the general form, Eq. (6), onto the $\hat{\mathbf{x}}$, $\hat{\mathbf{y}}$ (i.e., $\hat{\mathbf{k}}_\perp$, $\hat{\mathbf{z}} \wedge \hat{\mathbf{k}}_\perp$) plane becomes

$$\mathbf{K}_a = (\mathrm{Imag}\, K_{xx})\hat{\mathbf{x}}\hat{\mathbf{x}} + (\mathrm{Imag}\, K_{yy})\hat{\mathbf{y}}\hat{\mathbf{y}}$$

where

$$\mathrm{Imag} \begin{pmatrix} K_{xx} \\ K_{yy} \end{pmatrix} = \sum_j \frac{\omega_{pi,j}^2}{\omega^2} \int_0^\infty dv_\perp v_\perp^2 \frac{\partial f_{i,j}}{\partial v_\perp} \int_0^{2\pi} \frac{d\cos\theta}{(1 - k_\perp v_\perp \cos\theta/\omega + i\delta)} \begin{pmatrix} \cos^2\theta \\ \sin^2\theta \end{pmatrix} \quad , \tag{8a}$$

$$= \pi \sum_j \frac{\omega_{pi,j}^2 \omega}{k_\perp^2} \int_{v_\perp = \frac{\omega}{k_\perp}}^\infty dv_\perp \frac{\partial f_{i,j}}{\partial v_\perp} \begin{pmatrix} [(k_\perp^2 v_\perp^2) - \omega^2]^{-1/2} \\ [k_\perp^2 v_\perp^2) - \omega^2]^{1/2} \end{pmatrix} \quad . \tag{8b}$$

The normalizations of the various distribution functions which are consistent with Eqs. (7) and (8) are

$$\int_{-\infty}^{+\infty} dv_\parallel f_e(v_\parallel) = 1 \quad ,$$

and

$$\int_0^\infty dv_\perp v_\perp f_{i,j}(v_\perp) = \frac{1}{2\pi} \quad .$$

respectively.

By comparing the results, Eqs. (7) and (8) for the electron and ion contributions to wave damping, we note an important difference: Only those electrons which have $v_\parallel = \omega/k_\parallel$ exchange energy with the wave, whereas all ions with $v_\perp \geq \omega/k_\perp$ interact resonantly with a single wave. The difference arises because, during the course of their gyromotion,

$$\mathbf{v}_\perp(t) = v_\perp [\hat{\mathbf{x}}\, cos(\Omega_i t + \chi) - \hat{\mathbf{y}}\, sin(\Omega_i t + \chi)],$$

all such ions satisfy the resonance conditions $\omega - \mathbf{k}_\perp \cdot \mathbf{v}_\perp(t) = 0$ twice during each gyroperiod. The interaction with a narrow spectrum of lower hybrid waves will therefore perturb the electron distribution function in a similarly narrow region of velocity space, but will affect the ion distribution function over a much larger region.

Inclusion of **K** into the Maxwell's equations and eliminating **B** in favor of **E**, there results

$$\mathbf{n} \wedge (\mathbf{n} \wedge \mathbf{E}) + \mathbf{K} \cdot \mathbf{E} = 0 \tag{9}$$

with the definition $\mathbf{n} \equiv \mathbf{k}c/\omega$. Eq. (9) has a nontrivial solution for **E** if the dispersion relation

$$\varepsilon(\mathbf{k}, \omega) \equiv |\mathbf{n} \wedge (\mathbf{n} \wedge \mathbf{I}) + \mathbf{K}| = 0 \tag{10}$$

is satisfied. Explicitly, using Eqs. (5) in Eq. (10), we obtain

$$\varepsilon(\mathbf{k},\omega) = -K_{Th}(\frac{\omega}{c})^2 n_\perp{}^6 + [K_\perp n_\perp{}^2 + K_\parallel(n_\parallel{}^2 - K_\perp)]$$
$$(n^2 - K_\perp) + K_{xy}{}^2(n_\perp{}^2 - K_\parallel). \tag{11}$$

The extension of the local solutions Eq. (9) and Eq. (10) to a slowly varying plasma is accomplished by introducing the ray coordinate $\mathbf{r}$ and a parameter s upon which both $\mathbf{r}$ and $\mathbf{k}$ are assumed to depend.[11,12] Then, by expansion of the linearized field equations in the small quantity $|\nabla k|/k^2 \ll 1$, the equality (10) is maintained along the ray trajectories

$$\frac{d\mathbf{r}}{ds} = -\frac{\partial\varepsilon}{\partial\mathbf{k}}/\frac{\partial\varepsilon}{\partial s}, \quad \frac{d\mathbf{k}}{ds} = \frac{\partial\varepsilon}{\partial\mathbf{r}}/\frac{\partial\varepsilon}{\partial s}; \quad \frac{ds}{dt} = \frac{\partial\varepsilon}{\partial\omega}/\frac{\partial\varepsilon}{\partial s}. \tag{12}$$

The physical significance of the ray trajectory $\mathbf{r}[t(s)]$ and the streamline velocity $\mathbf{v}_{gr} = d\mathbf{r}/dt$ (the group velocity) is that the wave energy flux

$$\mathbf{F} = \mathbf{v}_{gr}U, \tag{13}$$

convects along $\mathbf{r}$. Here

$$U = \frac{1}{16\pi}(2\mathbf{E}^* \cdot \mathbf{K} \cdot \mathbf{E} + \omega\mathbf{E}^* \cdot \frac{\partial\mathbf{K}}{\partial\omega} \cdot \mathbf{E}) \tag{14}$$

is interpreted as the local wave energy density.

In solving the Hamiltonian system of ray equations [Eq. (12)], we make explicit use of the toroidal axisymmetry by transforming to canonical coordinates (r,θ,ϕ), with r the minor radial coordinate, θ the poloidal angle, and ϕ the toroidal angle; and to the conjugate momenta (k_r, m, n) in terms of which the wave vector becomes

$$\mathbf{k} = \hat{\mathbf{r}}k_r + \hat{\theta}\frac{m}{r} + \hat{\phi}\frac{n}{(R + r\cos\theta)}. \tag{15}$$

Since, by axisymmetry, $\partial\varepsilon/\partial\phi \equiv 0$, the conjugate momentum n is conserved for each ray. The six ray equations [Eq. (12)] then reduce to[14,15]

$$\frac{dr}{dt} = -\frac{\partial\varepsilon}{\partial k_r}/\frac{\partial\varepsilon}{\partial\omega}, \quad \frac{dk_r}{dt} = \frac{\partial\varepsilon}{\partial r}/\frac{\partial\varepsilon}{\partial\omega},$$
$$\frac{d\theta}{dr} = -\frac{\partial\varepsilon}{\partial m}/\frac{\partial\varepsilon}{\partial\omega}, \quad \frac{dm}{dt} = \frac{\partial\varepsilon}{\partial\theta}/\frac{\partial\varepsilon}{\partial\omega}, \tag{16}$$

which is the set we solve numerically.

Experimentally, the power spectrum incident on the plasma, $P(n_\parallel)$, is specified as a continuous function of the parallel index, $n_\parallel = k_\parallel c/\omega$, by controlling the size and relative phasing of the elements of a slow wave launching structure.[16] We separate the spectral shape function $S(n_\parallel)$ from the magnitude P_0, by writing

$$P(n_\parallel) = P_0 S(n_\parallel),$$

where

$$\int dn_{\parallel} S(n_{\parallel}) = 1.$$

Numerically, we approximate the continuous spectrum by apportioning the input energy flux amongst a sufficiently large number of discrete rays, each with launched power $P_j = P_0 S(n_{\parallel,j})\Delta n_{\parallel}$, so that the powers P_j vary reasonably smoothly as a function of ray index number j. The power convected by each ray satisfies the equation

$$\mathbf{v}_{gr,j} \cdot \nabla P_j = \gamma P_j, \tag{17}$$

where the (assumed small) damping decrement γ (< 0 for a stable plasma) is obtained by expanding Eq. (11) about $(\omega, \mathbf{k})$

$$\gamma = -\{\mathrm{Imag}\,\varepsilon[\mathbf{k}(\mathbf{r},\omega),\omega]\}/\frac{\partial \varepsilon}{\partial \omega}. \tag{18a}$$

Here

$$\mathrm{Imag}\,\varepsilon = \frac{\partial \varepsilon}{\partial K_{\parallel}} K_{\parallel,i} + \frac{\partial \varepsilon}{\partial K_{xx}} K_{xx,i} + \frac{\partial \varepsilon}{\partial K_{yy}} K_{yy,i}. \tag{18b}$$

IV. The Particle Kinetic Equations

A. General Observations

Some reduction in the dimensionality of the particle kinetic equations is necessary to make their solution tractable. To this end, we observe:

1) The electron and ion collision times are short compared to characteristic transport times, so that the steady-state solutions of the kinetic equations are adequate. We qualify this by noting that we should retain time dependence in the electron kinetic equation if runaway production in the combined presence of an inductive field and rf waves is to be properly treated. However, because the production of only a few runaways can effectively "short out" the inductive field, we need only check and be sure that the electric field strength being computed is below the value which produces runaways.

2) By virtue of the strong tokamak magnetic field, we may assume axisymmetry of all f_j about $\hat{\mathbf{b}} = \mathbf{B}/|\mathbf{B}|$ in velocity space, i.e., $f_j(\mathbf{v}) = f_j(v_{\perp}, v_{\parallel})$.

3) The collisional mean-free path is typically long compared to the convection length. Therefore, the electrons and the passing ions see an effective quasilinear diffusion coefficient equal to the flux surface average of the locally computed result, and the spatial dependence of the kinetic equations is reduced to a single (radial) coordinate.

B. Electrons

The reduced electron kinetic equation can be written

$$-(\frac{q}{m})\mathcal{E}\frac{\partial f}{\partial v_{\parallel}} = C(f) + W(f) + T(f). \tag{19}$$

Here $\mathcal{E}$ is the inductive electric field, $C(f)$ is the Coulomb collision operator, $W(f)$ is the wave diffusion operator, and $T(f)$ accounts for spatial transport of the electrons. Lacking a transport model, we replace $T(f)$ by the simple form

$$T(f) = -\nu_{Loss} f. \tag{20}$$

where the loss rate ν_{Loss} is to be associated with the experimentally determined particle confinement time. The wave diffusion operator is one-dimensional

$$W(f) = \frac{\partial}{\partial v_\parallel} D_{QL.e} \frac{\partial f}{\partial v_\parallel}. \tag{21}$$

The quasilinear diffusion coefficient is

$$D_{QL.e} = \frac{\pi}{2}\left(\frac{q}{m}\right)^2 \sum_j \langle |\mathbf{E}_j \cdot \hat{\mathbf{b}}|^2 \rangle \delta(\omega - k_{\parallel,j} v_\parallel), \tag{22}$$

where the sum is over all intersections by all rays with the flux surface under consideration and $\langle \quad \rangle$ denotes the flux surface average of the enclosed quantity. The required average $\langle |\mathbf{E}_j \cdot \hat{\mathbf{b}}|^2 \rangle$ can be related to the power P_j and the local polarization vector $\hat{\mathbf{e}}_j = \mathbf{E}_j/|\mathbf{E}_j|$, computed from Eqs. (9) and (17), respectively, by first observing that

$$P_j = \int_{A_\Psi} d\mathbf{S} \cdot \mathbf{F}_j = \int_{A_\Psi} d\mathbf{S} \cdot \mathbf{v}_{gr,j} U_j,$$

where the surface average covers the entire area A_Ψ of the flux surface under consideration, and then by using Eq. (14) for U_j, with the result

$$\langle |\mathbf{E}_j \cdot \hat{\mathbf{b}}|^2 \rangle = \frac{16\pi P_j}{|\mathbf{v}_{gr,j} \cdot \hat{\mathbf{r}}_j| A_\Psi} \hat{\mathbf{b}}\hat{\mathbf{b}} : \mathbf{Q}_j, \tag{23}$$

where

$$\mathbf{Q}_j = \frac{\mathbf{e}_j \mathbf{e}_j^*}{\mathbf{e}_j^* \cdot (2\mathbf{K} + \omega \partial \mathbf{K}/\partial \omega) \cdot \mathbf{e}_j}, \tag{24}$$

and $\hat{\mathbf{r}}_j$ is the normal to A_Ψ at the point where the j^{th} puncture occurs.

Solution of the full two-dimensional $(v_\parallel, v_\perp)$ Fokker-Planck equation [Eq. (19)] at even a single point and for a specified electric field requires considerable effort. Practically we are forced, without rigorous justification, to further reduction if kinetic effects are to be included at the transport level of description. We employ a one-dimensional collision operator of the form,

$$C(f) = \frac{\partial}{\partial v_\parallel}\left[\left(D_c \frac{\partial}{\partial v_\parallel} + \nu_c\right) f_e(v_\parallel)\right]. \tag{25}$$

The collisional diffusion and drag coefficients are given by

$$D_c = \nu_0 v_{Tc}{}^2 h(v_\parallel), \tag{26}$$

and

$$\nu_c = \nu_0 v_\parallel h(v_\parallel), \tag{27}$$

respectively, where

$$\nu_0 = \beta \frac{4\pi e^4 n}{m_e^2 v_{Te}^3} ln\Lambda,$$

and

$$h(v_\parallel) = \left[1 + (v_\parallel / v_{Te})^2\right]^{-3/2}.$$

The normalization coefficient β is chosen to yield the correct value for the electrical conductivity in the absence of rf. It is approximately $(1 + Z)/5$, with Z the ion charge. The form Eq. (25) has several desirable properties. Firstly, it conserves particle number. Secondly, the solution to $C(f) = 0$ is a Maxwellian (with thermal velocity v_{Te}). Finally, the velocity dependence of the coefficients are those obtained by expanding the linearized collision operator for high speeds $v \gg v_{Te}$. Eq. (25) can be "derived"[17] by averaging that operator over $v_\perp$, assuming f has a characteristic width $\Delta v_\perp \sim v_{Te}$.

One additional point deserves discussion. Referring back to the wave diffusion equation, we note that the discretization of the wave spectrum has made $D_{QL,e}$ singular. We resolve this singularity, and its counterpart in the expression, Eq. (7), for $K_{\parallel,e}$ by introducing a small but finite width δv into the wave-particle resonance. Specifically, we replace the delta function in Eqs. (7) and (22) with a Gaussian

$$\delta(\omega - k_\parallel v_\parallel) \rightarrow exp[-(\omega - k_\parallel v_\parallel)^2/2(\delta v)^2]/(2\pi)^{1/2}\delta v. \tag{28}$$

The size of δv is chosen large enough so that the convolving Gaussian spans several intervals $\Delta v_\parallel$ of the finite difference velocity grid on which f_e is solved.

C. Ions

Proceeding by analogy with the electron case, we treat the ion kinetic effects by averaging the full two-dimensional equation over $v_\parallel$, assuming a characteristic parallel velocity $v_\parallel \sim v_{T,i}$. We obtain, for $v_{Te} \gg v_\perp \gg v_{T,i}$,

$$0 = \frac{1}{v_\perp}\frac{\partial}{\partial v_\perp} v_\perp \{D_{QL,i}\frac{\partial f_i}{\partial v_\perp}(v_\perp) + D_{C,i}(\frac{\partial}{\partial v_\perp} + \frac{v_\perp}{{v_{T,i}}^2}) f_i(v_\perp)\}, \tag{29}$$

where, in this limit,[18]

$$D_{C,i}(v_\perp) = \frac{4\pi e^4 {v_{T,i}}^2}{m_i} ln\Lambda [\frac{1}{{v_\perp}^3}\sum_{j\neq e} n_j (\frac{1}{m_j} + \frac{1}{2m_i}) + \frac{1}{{v_{Te}}^3}(\frac{2}{\pi})^{1/2}\frac{n_e}{3m_e}]. \tag{30}$$

The sum is over all singly charged ion species j, each of density n_j and mass m_j. The quasilinear diffusion coefficient consistent with the wave-particle interaction discussed in Section III and used to compute the ion damping is

$$D_{QL,i}(v_\perp) = \frac{1}{2}\frac{q_i}{m_i^2}\sum_j [\hat{k}_j \hat{k}_j^* (\omega / k_{\perp,j} v_\perp)^2 (k_{\perp,j}^2 v_\perp^2 - \omega^2)^{-1/2}$$

$$+ (\hat{\mathbf{k}}_j \wedge \hat{\mathbf{b}})(\hat{\mathbf{k}}_j \wedge \hat{\mathbf{b}})^{\dagger}(k_{\perp,j}^2 v_\perp^2 - \omega^2)^{1/2}(k_{\perp,j} v_\perp)^{-2}] : \mathbf{Q}_j ;$$
$$v_\perp > \frac{\omega}{k_\perp}, \tag{31}$$

The first term results principally from the slow wave and the second from the fast wave. The sum is again over all punctures j of the flux surface Ψ.

Eq. (29) can be directly integrated. Prescribing the boundary condition that the velocity space flux vanishes and that f_i reduces to the bulk Maxwellian at small $v_\perp$ for which $D_{QL,i} = 0$, we obtain $f = f_{i,0}$, where

$$f_{i,0}(v_\perp) = \frac{n_i}{2\pi {v_{T,i}}^2} exp[-\frac{1}{{v_{T,i}}^2}\int_0^{v_\perp} dv_\perp' v_\perp'/(1 + D_{QL,i}/D_{C,i})]. \tag{32}$$

Because $D_{QL,i}$ is nonzero for all $v_\perp > \omega/k_\perp$, this solution typically contains an ion tail which extends to unphysically high energies. In a tokamak one expects that for velocities above some velocity v_{Loss} the ion orbits are unconfined, effectively truncating the distribution function at that velocity. Schuss has investigated the effects of loss due to trapping in toroidal ripples in the magnetic field strength.[19] We consider here the simpler case of an axisymmetric tokamak. We assume that the principal limitation on the confinement of very high energy trapped ions is that their banana width becomes large enough that they impact the limiter.

The calculation of the loss velocity can be done analytically.[20,21] Because of the assumed axisymmetry, the canonical angular momentum

$$p_\phi = mR^2\dot{\phi} + \frac{q}{c}RA_\phi \cong mRv_\parallel + \frac{q}{c}RA_\phi \tag{33}$$

is conserved. Here A_ϕ is the ϕ component of the magnetic vector potential, i.e., $\mathbf{B} = \nabla \wedge \mathbf{A}$, and $R = R_0 + r\cos\theta$ with R_0 the major tokamak radius. For a small aspect ratio tokamak, we have, to the required accuracy,

$$\mathbf{B} = \frac{R_0}{R}[\hat{\theta}B_\theta(r) + \hat{\phi}B_\phi], \tag{34}$$

with B_ϕ a constant. This form is generated by the vector potential

$$\mathbf{A} = R_0[\hat{\mathbf{z}}\, ln(\frac{R_0}{R})\, B_\phi - \frac{\dot{\phi}}{R}\int_0^r dr' B_\theta(r')]. \tag{35}$$

Combining p_ϕ with the two additional constants of the motion, the energy $T = (v_\perp^2 + v_\parallel^2)/2$ and the magnetic moment $\mu = v_\perp^2/B$, yields a relation for the perpendicular loss speed v_{Loss} above which ions of a given $v_\parallel$ injected at $\theta = 0$, $R = R_0 + r$ will impact the limiter at $R_a = R + a$ on their banana excursion. The result is

$${v_{Loss}}^2 = \{[Rv_\parallel + \frac{qR_0}{mc}\int_r^a dr' B_\theta(r')]^2 - (R_a v_\parallel)^2\}/R_a(a - r). \tag{36}$$

The loss process is incorporated into the ion kinetic equation by replacing the no-flux condition with the condition

$$f_i(v_\perp)|_{v_\perp = v_{Loss}} = 0. \tag{37}$$

In order to obtain a nontrivial steady-state solution, the velocity space flux implied by Eq. (37) is balanced by a source $S(v_\perp) = S_0\delta(v_\perp)/v_\perp$ where S_0 is to be determined. The solution for f_i is

$$f_i(v_\perp) = f_{i0}(v_\perp)\frac{H(v_\perp)}{H(0)}, \tag{38}$$

where

$$H(x) = \int_x^{v_{Loss}} dv_\perp'[1/v_\perp'(D_{QL\,i} + D_{C,i})]\,exp[\frac{1}{v_{Ti}^2}\int_{v_\perp}^{v_\perp'} dv_\perp'' v_\perp''/(1 + D_{QL,i}/D_{C,i})], \tag{39}$$

with $f_{i0}(v_\perp)$ given in Eq. (32).

V. Magnetic Flux Diffusion

The plasma current density obeys the deceptively simple equation

$$\frac{\partial j}{\partial t} = \frac{c^2}{4\pi}\frac{1}{r}\frac{\partial}{\partial r}r\frac{\partial \mathcal{E}}{\partial r} = \frac{c^2}{4\pi}\nabla_r^2\mathcal{E}, \tag{40}$$

when writen in terms of the inductive electric field $\mathcal{E}$. Boundary conditions appropriate to a small aspect ratio tokamak are

$$\frac{\partial \mathcal{E}}{\partial r}|_{r=0} = 0, \quad \mathcal{E}(a) + La\frac{\partial \mathcal{E}}{\partial r}|_{r=a} = \mathcal{E}_{ext}(t), \tag{41}$$

with L the plasma external inductance per unit length and $\mathcal{E}_{ext}$ the external electric field applied at $r = a$. In the presence of an rf-induced distortion of f_e, the explicit, linear relation $\mathcal{E} = \eta j$ is replaced by the implicit, nonlinear relation

$$j_{ke}(\mathcal{E}, r, t) = j(r, t), \tag{42}$$

where

$$j_{ke} = -qn\int_{-\infty}^{\infty} dv_\parallel v_\parallel f_e(v_\parallel, \mathcal{E}, r, t), \tag{43}$$

and f_e is the solution of the kinetic equation [Eq. (19)], assuming $D_{QL,e}$ is known.

An explicit (in time) finite difference solution of the parabolic equation [Eq. (40)] is inefficient because the time step required to ensure numerical stability is very small. Our approach is to linearize Eq. (40) about the solution computed at time t in advancing to $t + \Delta t$. We write, temporarily suppressing the spatial dependence,

$$\mathcal{E}(j^+) = \mathcal{E}(j^0) + \frac{\partial \mathcal{E}}{\partial j}(j^+ - j^0), \tag{44}$$

and solve the resulting implicit finite difference equation

$$j^+ - \frac{\Delta t\, c^2}{4\pi}\nabla_r^2[j^+\frac{\partial \mathcal{E}}{\partial j}(j^0,r,t)] = \frac{\Delta t\, c^2}{4\pi}\nabla_r^2[\mathcal{E}(j^0,r,t) - j^0\frac{\partial \mathcal{E}}{\partial j}(j^0,r,t)], \qquad (45)$$

for j^+. Upon obtaining j^+, the implicit equation [Eq. (42)] is solved at each radial point r_j for a new set $\{\mathcal{E};\, \partial\mathcal{E}/\partial j\}$ by employing a Newton root finding technique and putting $j(r,t) = j^+(r_j)$ there. The procedure works well except when the rf power is changed discontinuously in time. (We will discuss this more difficult situation below.)

The current density profiles generated by this model are generally narrower than the experimentally inferred profiles[4] and tend to peak away from the minor axis. The latter effect is a consequence of the fact that none of the rays penetrate completely to the minor axis. The narrow profiles are to be expected because we have neglected smoothing effects, which include M.H.D. activity inside the $q = 1$ surface and energetic electron transport. Transport is especially important in machines such as PLT where the energetic electron collisional slowing down time is not very much shorter than the particle confinement time. For instance, taking a confinement time $\tau \sim 50\,\mathrm{msec}$ and attributing the loss to a diffusive process, we find that under conditions appropriate for current drive in PLT, $n \sim 10^{13}\,\mathrm{cm}^{-3}$, $T_{tail} \sim 50\,\mathrm{keV}$, the tail electrons diffuse a distance comparable to the minor radius as they slow down. (For a reactor-sized experiment, the effects of diffusion will be less pronounced.) We have incorporated some features of electron transport in a heuristic way by making the replacement

$$\mathcal{E} \to \mathcal{E} - \frac{4\pi}{\omega_{pe}^2}\nabla\cdot D_J\nabla j\,, \qquad (46)$$

in Eq. (40). The diffusion coefficient D_J is related to the characteristic confinement time by $D_J \sim a^2/\pi^2\tau$.

VI. Applications

The modeling code is used to calculate steady-state and ramp-up current drive as well as the effect of ion absorption on current drive. We will present some ramp-up and ion absorption results done for the PLT tokamak. In these calculations the current density is the only transport quantity which is evolved. The number density and temperature profiles are fixed and have an assumed form

$$A(r) = [A(0) - A(a)][p(r)]^{\gamma_A} + A(a)\,, \qquad (47)$$

where the radial function $p(r) = 1 - (r/a)^2$, and where a is the minor radius.

At the initial time $t = 0$, the rf power is set to zero. The initial current profile is obtained by specifying the total plasma current I and by assuming a steady-state ohmic discharge, $\partial\mathcal{E}/\partial r = 0$. Eq. (42) is iterated until the value of $\mathcal{E}$ which produces the specified current is obtained. At some later time $t = t_1$, the rf is instantaneously

turned on. Since we solve the steady-state kinetic equations, a numeric algorithm is required to mimic the relaxation of the distribution functions and of the spectrum which physically occurs in a time of the order of the energetic particle collision time. We address this issue by employing the following iteration procedure: The rf power is first set to a small fraction ($\sim 10^{-3}$) of its ultimate value, and the powers P_j are computed using the unperturbed f_j. Given these initial $P_j(r)$, new f_j are calculated. The process is repeated, typically 10 times. At each step, the applied power is increased by a roughly constant factor until the prescribed power is attained. Good convergence is obtained for all quantities. At subsequent times $t > t_1$, good results are obtained with only a single iteration since the time behavior is smooth.

The quantities $\hat{\mathbf{e}}$, $v_{gr,r}$, $\theta(r)$, $n_\parallel$, $\mathbf{n}_\perp$ are required in order to compute the wave-particle interaction. They are computed and stored for each ray at each crossing of a radial zone. Since the temperature and density profiles are fixed, and since the fractional current change is $\leq 15\%$ in the ramp-up case, we have evaluated these quantities once only, at the initial time $t = 0$.

An important parameter for electron absorption, and thus current drive, is the parallel phase velocity of the wave, often expressed in terms of the parallel index of refraction $n_\parallel = k_\parallel c/\omega$. In toroidal geometry $n_\parallel$ is not a constant and can change significantly from the launched value. This is important for PLT since the launched waves have parallel phase velocities that are too large to interact with the electrons. The value of $n_\parallel$ along the trajectory given in Fig. 1 is shown in Fig. 2. On the first pass $n_\parallel$ is approximately constant, but after one wall reflection $n_\parallel$ increases sufficiently so that the power in that ray is absorbed near the center of the plasma. The trajectories and $n_\parallel$ shifts depend on the plasma current and density profiles. For a large range of current and density the inclusion of multiple wall reflections results in sufficient $n_\parallel$ shifts so that a significant fraction of the launched power is absorbed. For very low densities, such as discussed below for the current ramp-up calculations, an additional small shift of launch spectrum to larger $n_\parallel$ is sometimes needed to obtain sufficient power absorption. Possible physical justifications for this additional shift are scattering from drift waves[22,23] and/or wall imperfections.

A. Ramp-Up

The modeling code allows the simulation of current ramp-up including the effect of the inductive electric field which opposes the ramp-up. An important question is what fraction of the input rf power goes into increasing the poloidal magnetic field. This is a measure of the ramp-up efficiency. The dependence of this fraction on input power has been calculated and compares favorably with experiments.[24] We will give some details for a relatively high power case where the back inductive electric field is important in calculating the ramp-up efficiency.

The input power is 300 kW launched into a plasma with an initial current of 180 kA. The average electron density is $3 \times 10^{12}\text{cm}^{-3}$ and the center temperature

is 1.25 keV. The calculation is run for a time interval of 0.5 sec. After 0.25 sec. the increase in current is approximately constant at $50\,\mathrm{kAs}^{-1}$. The initial and final current profiles are given in Fig. 3, along with the initial and final electric field. The electric field on axis at 0.5 sec is approximately equal (with the opposite sign) to the initial field which produced the starting current of 180 kA. The effect of this electric field is seen in Fig. 4, where the distribution is skewed on the negative velocity side. The plateau on the positive velocity side is the rf-generated tail which is carrying the plasma current. The effect of the electric field is decreased for a larger Z_{eff} since the collisional diffusion and drag coefficients are increased. This is seen in Fig. 5 for Z_{eff} of 3. It is clearly seen that in both cases the distribution is far from Maxwellian, and therefore, a calculation including quasilinear absorption is essential. The fractions of input power going into increasing the poloidal field are 0.14 and 0.19 for a Z_{eff} of 1 and 3, respectively.

B. Minority Absorption

It has been observed on a number of machines that above a critical density, current drive efficiency rapidly decreases.[2,25,26] On PLT this *density limit* is observed to occur at an average electron density of order $0.8 - 0.9 \times 10^{13}\mathrm{cm}^{-3}$ for a plasma current of 200 kA .[27] This density is significantly below the density for mode conversion where the perpendicular phase velocity of the waves becomes comparable to the thermal velocity of the bulk deuterium ions. However, a light minority ion species, such as hydrogen, can interact with the lower hybrid waves at this density. There are two major questions remaining: first, are there enough hydrogen ions, and second, are they contained well enough to absorb a significant fraction of the input power. We will summarize the results of the calculations done for PLT.[8,28] We note that minority hydrogen absorption has been independently suggested as a cause for the density limit on the FT tokamak.[26] However, these calculations did not consider the confinement of the hydrogen tail.

The amount of hydrogen present in PLT when the density limit was measured can only be estimated. Values of $10 - 25\%$ are considered possible.[29] We present results for 10% and 25% hydrogen in a deuterium plasma. Figure 6 gives the percentage of the total power which was absorbed by the hydrogen ions for average electron densities between 0.7 and $1 \times 10^{13}\mathrm{cm}^{-3}$. When the hydrogen ions are absorbing greater than 50% of the power, current drive is strongly affected. This occurs for 25% hydrogen at densities greater than $\sim 0.9 \times 10^{13}\mathrm{cm}^{-3}$, and is consistent with the experiments. For 10% hydrogen only $\sim 20\%$ is absorbed by the hydrogen ions at $1 \times 10^{13}\mathrm{cm}^{-3}$. These results are for a plasma current of 200 kA. The absorption by hydrogen is strongly affected by the value of ν_{Loss}, Eq. (36), which depends on the plasma current through the poloidal magnetic field. Rather than change the current which also affects absorption through changes in ray trajectories, we explored the effect of doubling ν_{Loss} as calculated at each radial point from Eq. (36). This also explores the question as to whether or not at a given current, ion banana

losses are reduced by other effects such as collisions. The result for 10% hydrogen is given in Fig. 6, where one observes that greater than 50% of the power goes to ions for densities greater than $\sim 0.9 \times 10^{13}\text{cm}^{-3}$. The effect of changing v_{Loss} is clearly seen in Figs. 7 and 8, where contours of the ion distribution as a function of perpendicular velocity and radius are given. Note that as v_{Loss} increases, the tail extends out to larger velocity and increases in size. We conclude that if there is 25% hydrogen ions (or if there is less hydrogen that is better contained than that calculated by our simple banana losses model), the minority hydrogen ions can play a role in explaining the observed density limit on PLT.

VII. Conclusions

We have described a lower hybrid modeling code, LHMOD, which solves the tightly coupled equations of lower hybrid heating and current drive in a toroidal plasma. In developing the code, we have attempted to balance the need to treat each physical process in sufficient detail with the need to work at the transport level of description. The propagation of the waves is treated in the ray approximation with an assumed small damping decrement. (The anti-Hermetian part of the dielectric tensor is calculated as a correction term.) Quasilinear theory is required to calculate the damping and the resulting non-Maxwellian electron and ion velocity distribution functions. The kinetic effects are simplified by using one-dimensional collision operators for both the electrons and ions. The dominant ion loss mechanism is assumed to result from extended banana orbits which impact the limiter. Finally, the plasma current is advanced in time by an implicit scheme which includes some effects of electron transport.

The evolution of the current profile is shown for a ramp-up case on the PLT tokamak where approximately 14% of the launched 300 kW of rf power goes into increasing the poloidal field. The back inductive electric field plays an important role at this power level. The effect of the electric field is decreased and the fraction of power going into increasing the poloidal field is increased if Z_{eff} is increased. Another example application of the code, to a determination of the role of minority hydrogen ion absorption in explaining the density limit, is discussed.

ACKNOWLEDGMENTS

We are grateful for informative discussions with P. Bonoli, R. Englade, and N. Fisch, and to C. Karney whose suggestions at the initiation of this effort were quite helpful. We appreciate the efforts of S. Bernabei, T. K. Chu, W. Hooke, F. Jobes, R. Motley, and J. Stevens in making PLT data readily available to us and also for many informal discussions about the experiments.

This work was supported by the United States Department of Energy under Contract DE-AC02-76-CHO-3073.

References

[1]N. J. Fisch, Phys. Rev. Lett. **41**, 873 (1978).

[2]S. Bernabei, C. Daughney, P. Efthimion, W. Hooke, J. Hosea, F. Jobes, A. Martin, E. Mazzucato, E. Meservey, R. Motley, J. Stevens, S. von Goeler, and R. Wilson, Phys. Rev. Lett. **49**, 1255 (1982).

[3]M. Porkolab, J. J. Schuss, B. Lloyd, Y. Takase, S. Texter, P. Bonoli, C. Fiore, R. Gandy, D. Gwinn, B. Lipshultz, E. Marmar, D. Pappas, R. Parker, and P. Pribyl. Phys. Rev. Lett. **53**, 450 (1984).

[4]W Hooke, Plasma Phys. and Contr. Fusion **26(1A)**, 133 (1984).

[5]D. A. Ehst, C. D. Boley, K. Evans, J. Jung, C. A. Trachsel, T. Hino, J. Fusion Energy **2**, 83 (1982).

[6]Tokamak Fusion Core Experiment Preconceptual Design Report, Princeton University Plasma Physics Laboratory, June 1984 (unpublished).

[7]C. F. F. Karney, and N. J. Fisch, Phys. Fluids **29**, 180 (1986).

[8]D. C. Eder, E. J. Valeo, S. Bernabei, and J. Stevens, Bull. Am. Phys. Soc. **28**, 1090 (1983); D. C. Eder, E. J. Valeo, and F. Jobes, *ibid.*, **29**, 1366 (1984).

[9]P. Bonoli, R. Englade, and M. Porkolab, MIT Plasma Fusion Center Rept. PFC/CP-84-6, March, 1984.

[10]T. H. Stix, *The Theory of Plasma Waves* (McGraw-Hill, New York, 1962).

[11]S. Weinberg, Phys. Rev. **126**, 1899 (1962).

[12]I. B. Bernstein, Phys. Fluids **18**, 320 (1975).

[13]C. F. F. Karney, Phys. Fluids **22**, 2188 (1979).

[14]E. Ott, J. M. Wersinger, and P. T. Bonoli, Phys. Fluids **22**, 192 (1979).

[15]D. W. Ignat, Phys. Fluids **24**, 1110 (1981).

[16]M. Brambilla, Nucl. Fusion **16**, 47 (1976).

[17]C. F. F. Karney and N. J. Fisch, Phys. Fluids **22**, 1817 (1979).

[18]B. A. Tribnikov, in *Reviews of Plasma Physics*, edited by Leontovich, M. A., (Consultants Bureau, New York, 1965), Vol. 1, page 105.

[19]J. J. Schuss, T. M. Antonsen, and M. Porkolab, Nucl. Fusion **23**, 201 (1983).

[20]J. A. Rome, D. G. McAlees, J. D. Callen, and R. H. Fowler, Nucl. Fusion **16**, 55 (1976).

[21]L. M. Hively and G. H. Miley, Nucl. Fusion **17**, 1031 (1977).

[22]P. L. Andrews, and F. W. Perkins, Phys. Fluids **26**, 2537 (1983); *ibid.*, 2546 (1983).

[23]P. L. Andrews, V. S. Chan, and C. S. Liu, Phys. Fluids **28**, 1148 (1985).

[24]F. W. Perkins, *et al.*, Proc. of Tenth IAEA Intl. Conf. on Plasma Physics and Contr. Nucl. Fusion Res., London, UK, Vol. I, p. 513, September 1984.

[25]S. C. Luckhardt, M. Porkolab, S. F. Knowlton, K. I. Chen, A. S. Fisher, F. S. McDermott, and M. Mayberry, Phys. Rev. Lett. **48**, 152 (1982).

[26]FT Group, EURATOM-ENEA Report 83.38, November, 1983.

[27]J. E. Stevens, *et al.*, Proc. of 3rd Joint Varenna-Grenoble International Symposium, Vol. II, p. 455, March, 1982.

[28]D. C. Eder, and E. J. Valeo, (unpublished).

[29]W. M. Hooke, private communication, (1984).

Figures

FIG. 1. Ray trajectory $r(\theta)$ for outside launch. The first (resp. second) pass is shown as a solid (resp. dashed) curve. The plasma parameters are: $n_e(0) = 10^{13}\,\mathrm{cm}^{-3}$, $n_e(a) = 10^{12}\,\mathrm{cm}^{-3}$, $\gamma_{n_e} = 1$, $R = 133\,\mathrm{cm}$, $a/R = 0.3$, $I = 200\,\mathrm{kA}$, $B_\phi = 29\,\mathrm{kG}$, $T_e(0) = 1.25\,\mathrm{keV}$, $T_e(a) = 100\,\mathrm{eV}$, $\gamma_{T_e} = 3.0$, $T_i(0) = 0.8\,\mathrm{keV}$, $T_i(a) = 100\,\mathrm{eV}$, $\gamma_{T_i} = 2$.

FIG. 2. Parallel index $n_\parallel$ versus minor radial position r for the trajectory of Fig. 1.

FIG. 3. Initial (i, $t = 0$) and final (f, $t = 500\,\mathrm{msec}$) profiles of the inductive electric field $\mathcal{E}$ and current density j for current ramp-up simulation with parameters: $P_{rf} = 300\,\mathrm{kW}$ turned on at $t = 100\,\mathrm{msec}$, launched from the outside. Input spectrum is peaked at $n_\parallel = 2.4$ and has a width $\Delta n_{\parallel\,FWHM} = 1.2$, $I(t = 0) = 180\,\mathrm{kA}$, $n_e(0) = 4.5 \cdot 10^{12}\,\mathrm{cm}^{-3}$, $n_e(a) = 6 \cdot 10^{11}\,\mathrm{cm}^{-3}$, $\gamma_{n_e} = 1$, $\mathrm{Z_{eff}} = 1$. Other parameters are as for Fig 1. The rays make approximately 5 full radial passes, after which 40% of the launched power is absorbed.

FIG. 4. Level countour of $f_e(v_\parallel, r)$ at $t = 500\,\mathrm{msec}$ for the parameters of Fig. 3 which shows the rf-generated quasilinear plateau for $v_\parallel > 0$ and the acceleration of electrons to $v_\parallel < 0$ near $r = 0$ by the opposing inductive electric field (see Fig. 2).

FIG. 5. Level contour of $f_e(v_\parallel, r)$ with all parameters as in Figs. 3 and 4, except $\mathrm{Z_{eff}} = 3$. The larger $\mathrm{Z_{eff}}$ results in a less pronounced negative velocity tail near $r = 0$.

FIG. 6. Absorption P_H due to hydrogen minority as compared to the sum P_{TOT} of electron and ion absorption vs. line average density $\bar{n}_e$ for 10% ($\bullet$) and 25% ($\circ$) minority concentration and for 10% concentration with $v_{Loss} = 2v_{Loss}$ ($\times$). Other parameters: The same as for Fig.(1), except $P_{rf} = 200\,\mathrm{kW}$, $n_e(a) = 0.1 \cdot n_e(0)$, max $S(n_\parallel)$ at $n_\parallel = 2$, $\Delta n_{\parallel\,FWHM} = 1$.

FIG. 7. Level curves of minority hydrogen distribution function $f_i(v_\perp, r)$, showing quasilinear tail associated with absorption. The loss velocity v_{Loss} used in boundary condition Eq. (39) is computed from Eq. (36). Parameters: $n_{Hydrogen} = 0.1 \cdot n_{Deuterium}$, $n_e(0) = 1.35 \cdot 10^{13}\,\mathrm{cm}^{-3}$, otherwise as in Fig. (6).

FIG. 8. Same as Fig (7) except that v_{Loss} is double the value given by Eq. (36).

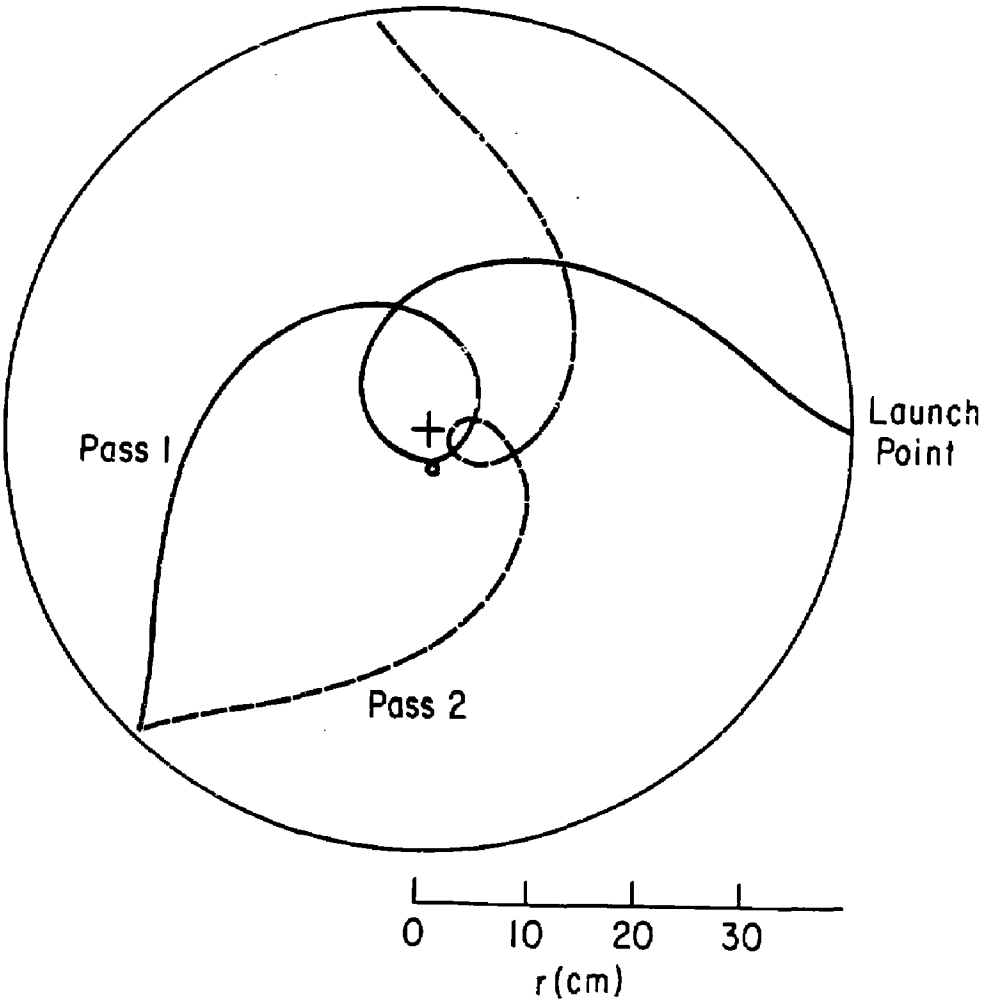

Fig. 1

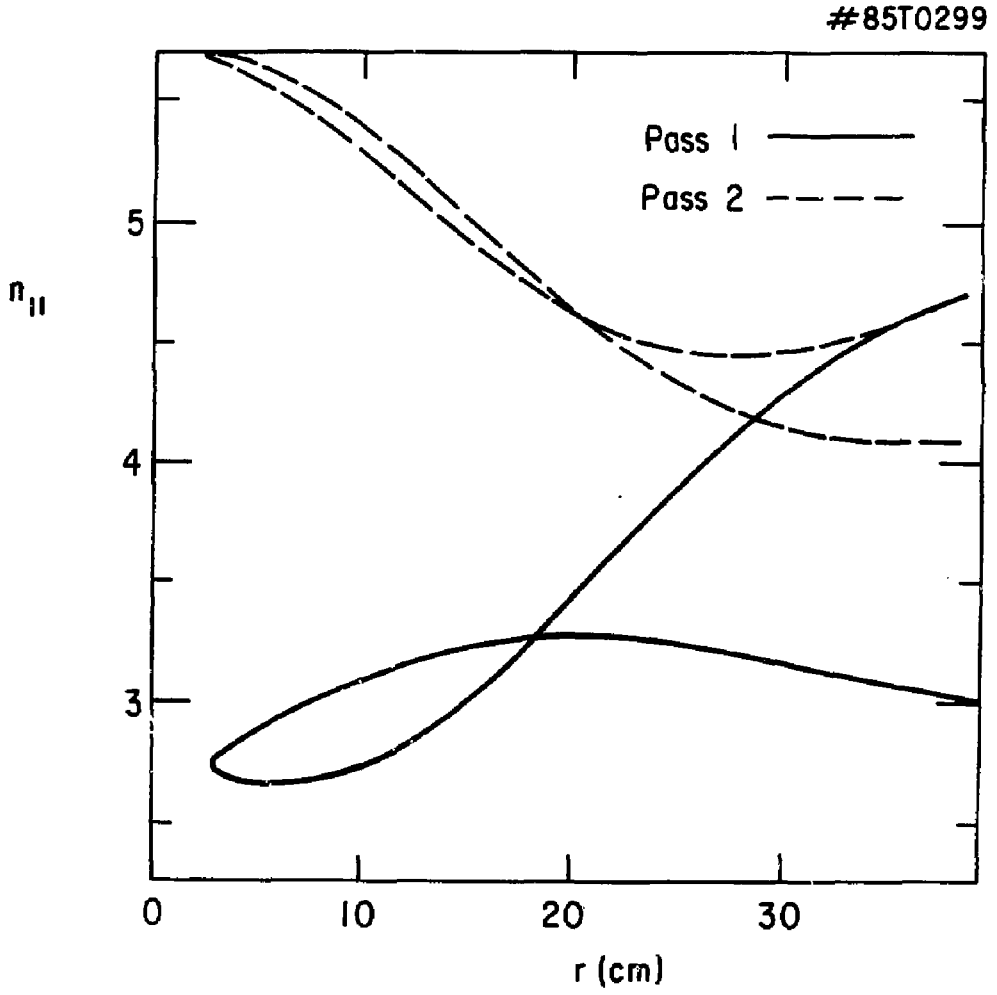

Fig. 2

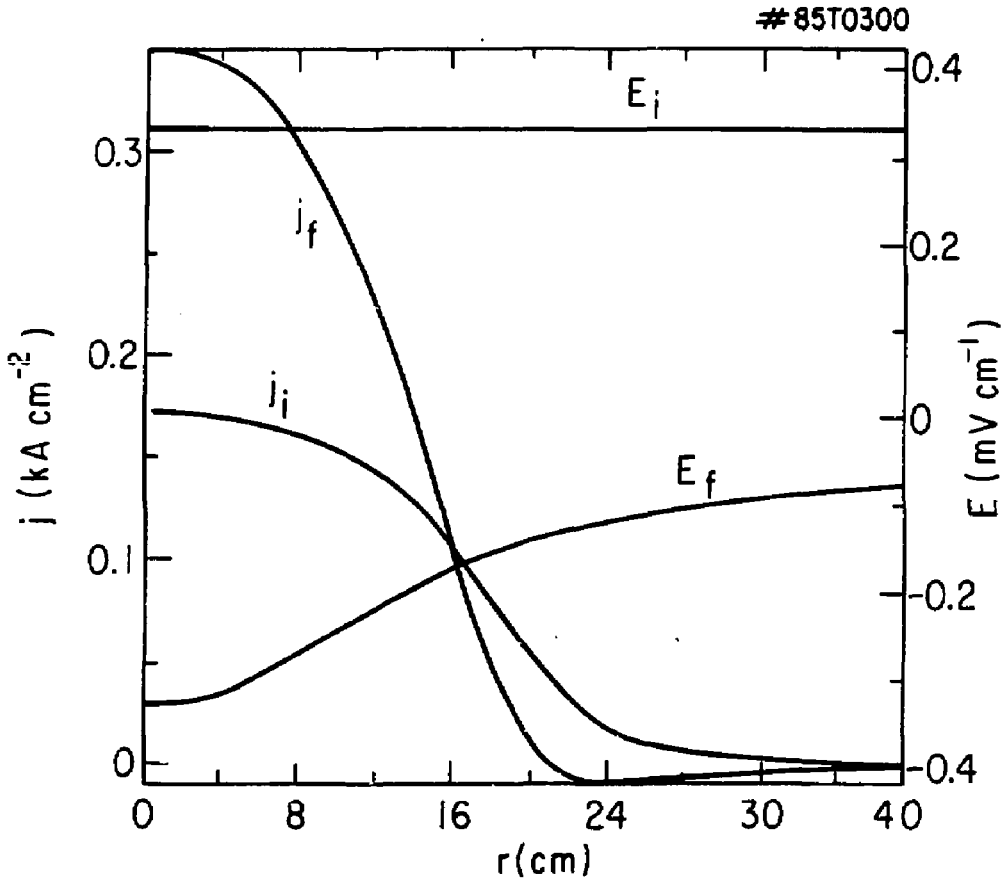
#85T0300
E_i
j_f
j_i
E_f
j (kA cm^{-2})
E (mV cm^{-1})
r(cm)
0
8
16
24
30
40
0.3
0.2
0.1
0
0.4
0.2
0
-0.2
-0.4

Fig. 3

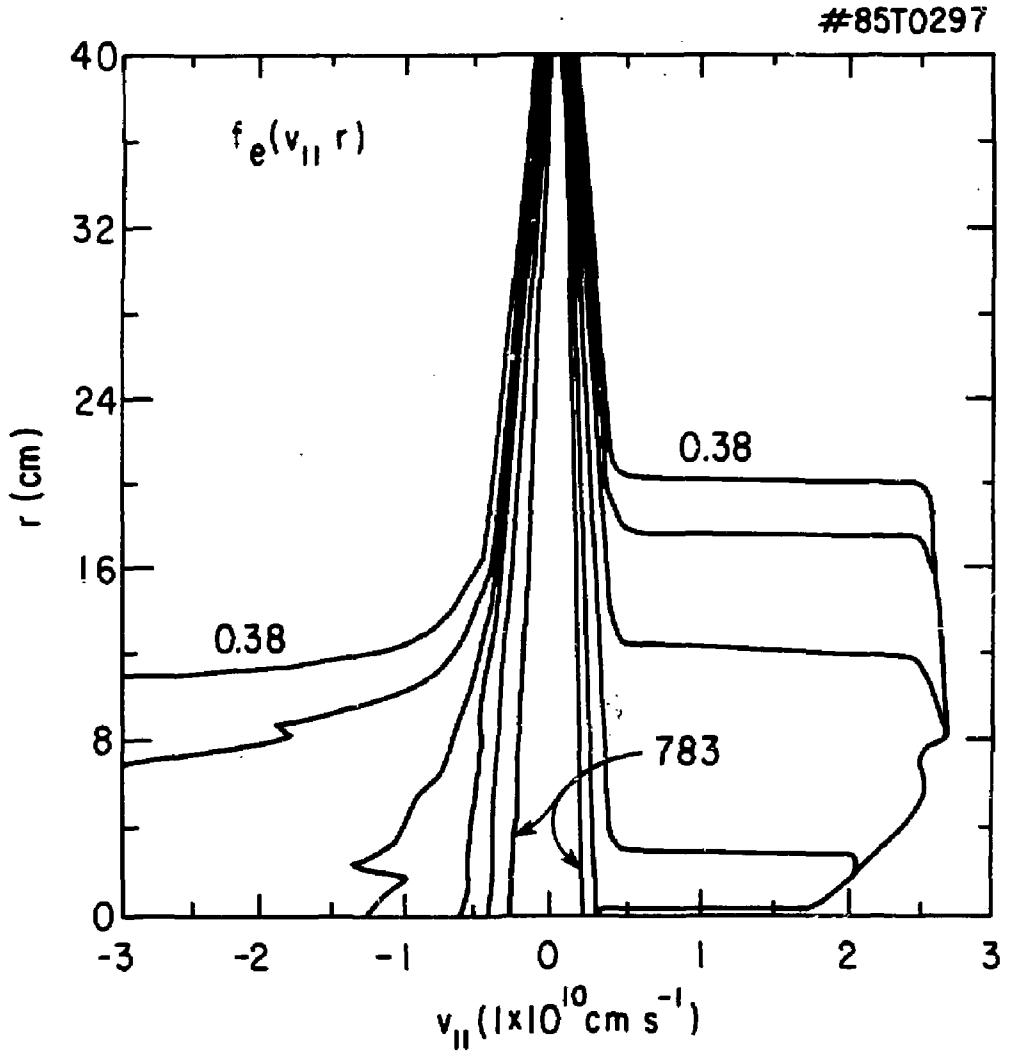
#85T0297
$f_e(v_{||}\, r)$
40
32
24
16
8
0
r (cm)
0.38
0.38
783
-3
-2
-1
0
1
2
3
$v_{||}(1\times10^{10}\,cm\,s^{-1})$

Fig. 4

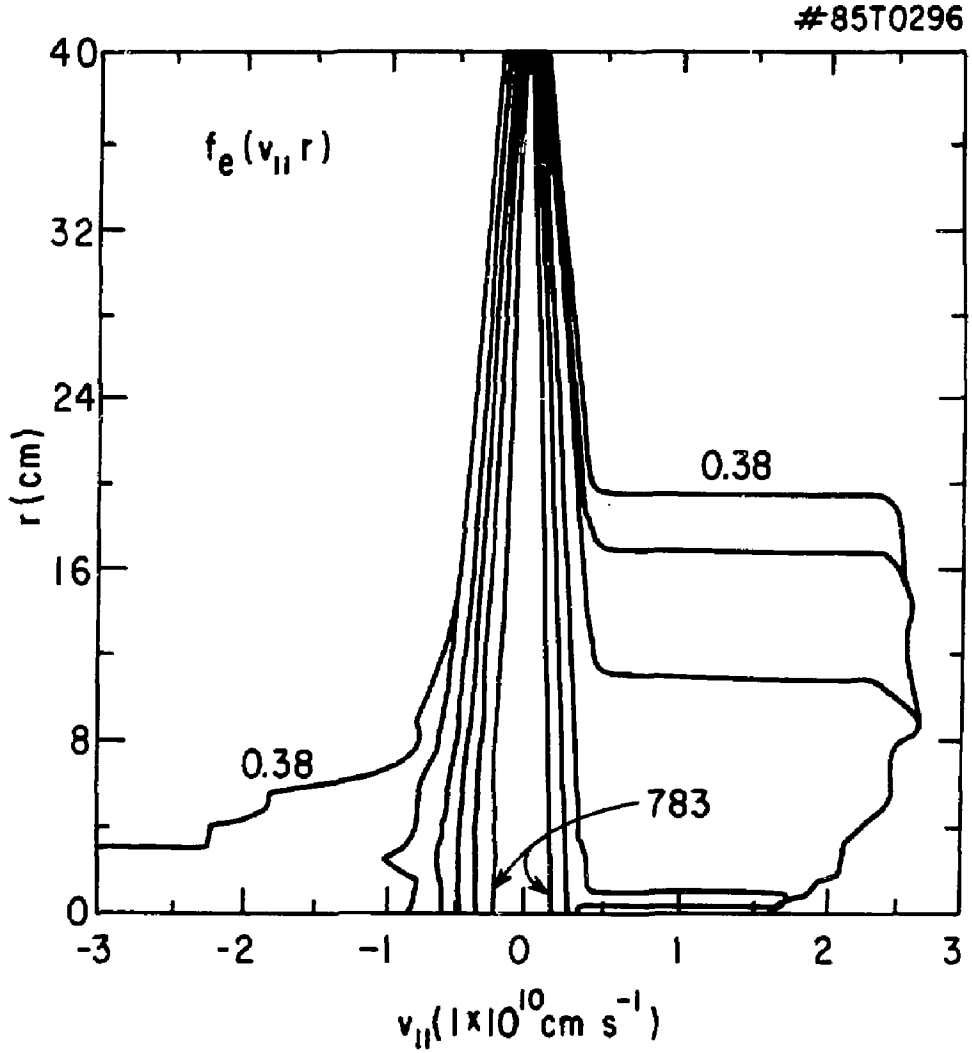
#85T0296
40
32
24
16
8
0
r(cm)
$f_e(v_{||} r)$
0.38
0.38
783
-3
-2
-1
0
1
2
3
$v_{||}(1 \times 10^{10} cm\ s^{-1})$

Fig. 5

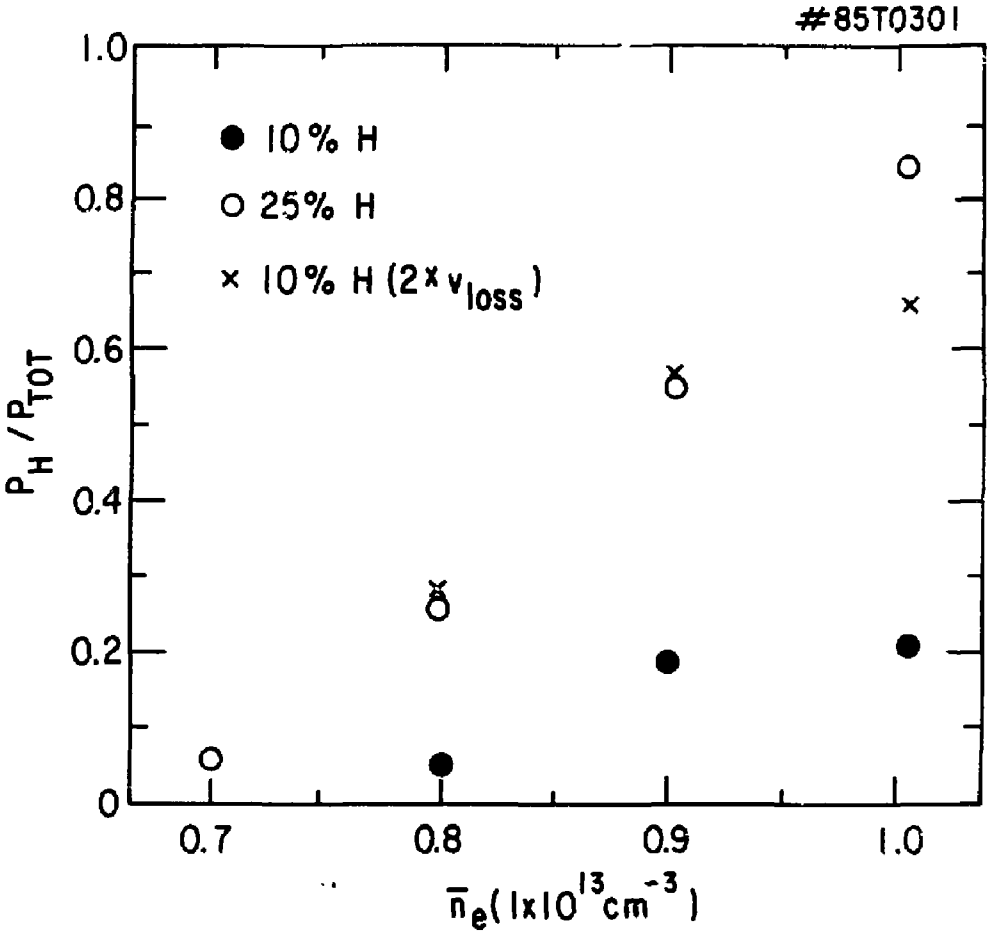
#85T0301
1.0
0.8
0.6
0.4
0.2
0
● 10% H
○ 25% H
× 10% H (2× v_{loss})
P_H / P_{TOT}
0.7
0.8
0.9
1.0
$\bar{n}_e (1 \times 10^{13} cm^{-3})$

Fig. 6

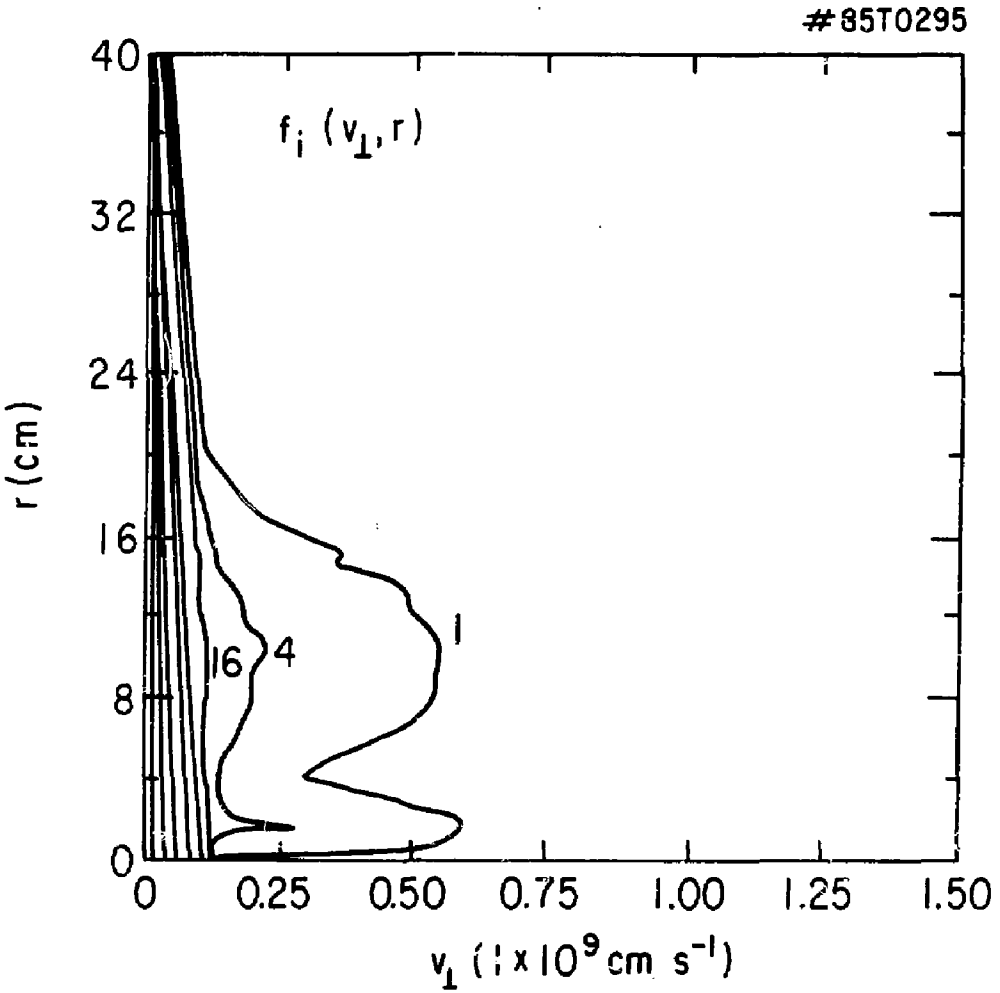
#85T0295
40
32
24
16
8
0
r (cm)
$f_i (v_\perp, r)$
1
4
16
0
0.25
0.50
0.75
1.00
1.25
1.50
$v_\perp$ ($\times 10^9$ cm s^{-1})

Fig. 7

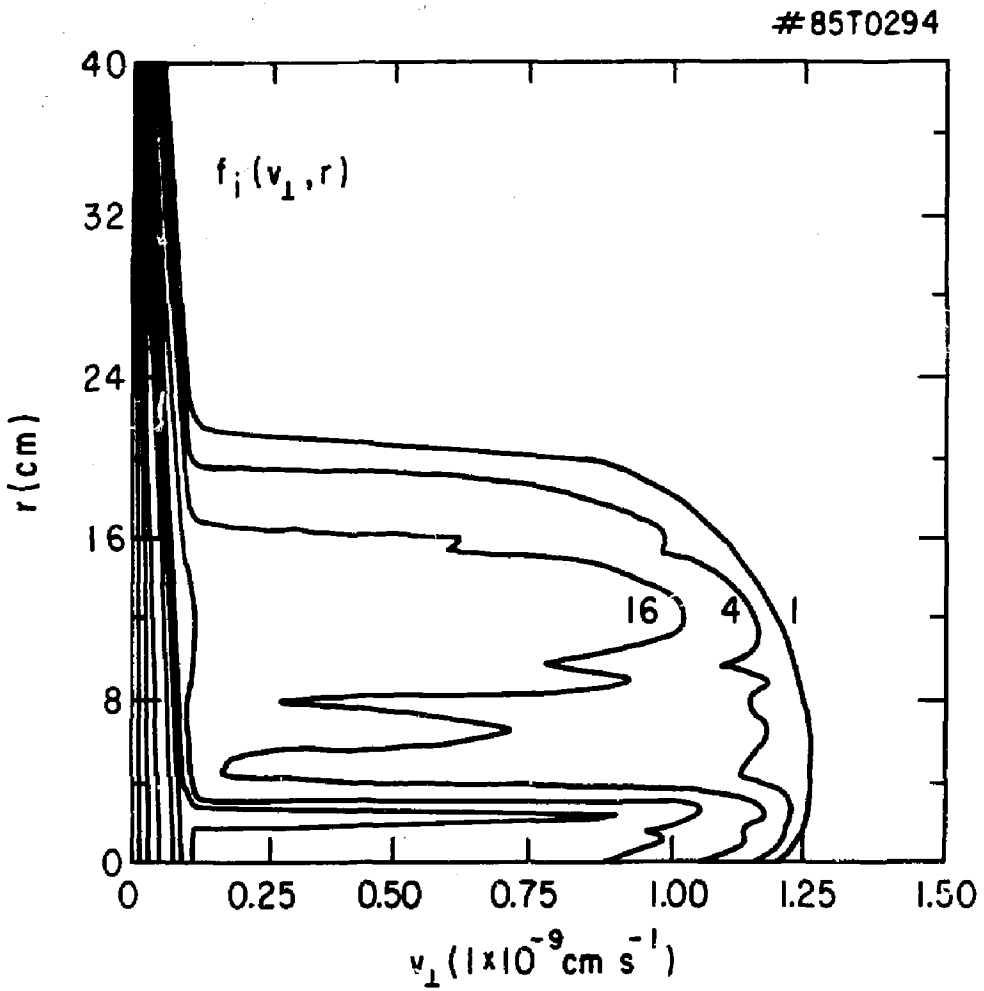
#85T0294
$f_i(v_\perp, r)$
r(cm)
40
32
24
16
8
0
16
4
1
0
0.25
0.50
0.75
1.00
1.25
1.50
$v_\perp (1 \times 10^{-9} cm\ s^{-1})$

Fig. 8

EXTERNAL DISTRIBUTION IN ADDITION TO UC-20

Plasma Res Lab, Austra Nat'l Univ, AUSTRALIA
Dr. Frank J. Paoloni, Univ of Wollongong, AUSTRALIA
Prof. I.R. Jones, Flinders Univ., AUSTRALIA
Prof. M.H. Brennan, Univ Sydney, AUSTRALIA
Prof. F. Cap, Inst Theo Phys, AUSTRIA
Prof. Frank Verheest, Inst theoretische, BELGIUM
Dr. D. Palumbo, Dg XII Fusion Prog, BELGIUM
Ecole Royale Militaire, Lab de Phys Plasmas, BELGIUM
Dr. P.H. Sakanaka, Univ Estadual, BRAZIL
Dr. C.R. James, Univ of Alberta, CANADA
Prof. J. Teichmann, Univ of Montreal, CANADA
Dr. H.M. Skarsgard, Univ of Saskatchewan, CANADA
Prof. S.R. Sreenivasan, University of Calgary, CANADA
Prof. Tudor W. Johnston, INRS-Energie, CANADA
Dr. Hannes Barnard, Univ British Columbia, CANADA
Dr. M.P. Bachynski, MPB Technologies, Inc., CANADA
Chalk River, Nucl Lab, CANADA
Zhengwu Li, SW Inst Physics, CHINA
Library, Tsing Hua University, CHINA
Librarian, Institute of Physics, CHINA
Inst Plasma Phys, Academia Sinica, CHINA
Dr. Peter Lukac, Komenskeho Univ, CZECHOSLOVAKIA
The Librarian, Culham Laboratory, ENGLAND
Prof. Schatzman, Observatoire de Nice, FRANCE
J. Radet, CEN-BP6, FRANCE
AM Dupas Library, AM Dupas Library, FRANCE
Dr. Tom Mual, Academy Bibliographic, HONG KONG
Preprint Library, Cent Res Inst Phys, HUNGARY
Dr. R.K. Chhajlani, Vikram Univ. INDIA
Dr. B. Dasgupta, Saha Inst, INDIA
Dr. P. Kaw, Physical Research Lab, INDIA
Dr. Phillip Rosenau, Israel Inst Tech, ISRAEL
Prof. S. Cuperman, Tel Aviv University, ISRAEL
Prof. G. Rostagni, Univ Di Padova, ITALY
Librarian, Int'l Ctr Theo Phys, ITALY
Miss Clelia De Palo, Assoc EURATOM-ENEA, ITALY
Biblioteca, del CNR EURATOM, ITALY
Dr. H. Yamato, Toshiba Res & Dev, JAPAN
Direc. Dept. Lg. Tokamak Dev. JAERI, JAPAN
Prof. Nobuyuki Inoue, University of Tokyo, JAPAN
Research Info Center, Nagoya University, JAPAN
Prof. Kyoji Nishikawa, Univ of Hiroshima, JAPAN
Prof. Sigeru Mori, JAERI, JAPAN
Prof. S. Tanaka, Kyoto University, JAPAN
Library, Kyoto University, JAPAN
Prof. Ichiro Kawakami, Nihon Univ, JAPAN
Prof. Satoshi Itoh, Kyushu University, JAPAN
Dr. D.I. Choi, Adv. Inst Sci & Tech, KOREA
Tech Info Division, KAERI, KOREA
Bibliotheek, Fom-Inst Voor Plasma, NETHERLANDS
Prof. B.S. Liley, University of Waikato, NEW ZEALAND
Prof. J.A.C. Cabral, Inst Superior Tecn, PORTUGAL
Dr. Octavian Petrus, ALI CUZA University, ROMANIA
Prof. M.A. Hellberg, University of Natal, SO AFRICA
Dr. Johan de Villiers, Plasma Physics, Nucor, SO AFRICA
Fusion Div. Library, JEN, SPAIN
Prof. Hans Wilhelmson, Chalmers Univ Tech, SWEDEN
Dr. Lennart Stenflo, University of UMEA, SWEDEN
Library, Royal Inst Tech, SWEDEN
Centre de Recharcheesn, Ecole Polytech Fed, SWITZERLAND
Dr. V.T. Tolok, Khadtov Phys Tech Ins, USSR
Dr. D.D. Ryutov, Siberian Acad Sci, USSR
Dr. G.A. Eliseev, Kurchatov Institute, USSR
Dr. V.A. Glukhikh, Inst Electro-Physical, USSR
Institute Gen. Physics, USSR
Prof. T.J.M. Boyd, Univ College N Wales, WALES
Dr. K. Schindler, Ruhr Universitat, W. GERMANY
Nuclear Res Estab, Julich Ltd, W. GERMANY
Librarian, Max-Planck Institut, W. GERMANY
Bibliothek, Inst Plasmaforschung, W. GERMANY
Prof. R.K. Janev, Inst Phys, YUGOSLAVIA